Conjugated polymer-fullerene blend with strong optical limiting in the near-infrared

San-Hui Chi, Joel M. Hales, Matteo Cozzuol, Charles Ochoa, Madison Fitzpatrick, and Joseph W. Perry*

School of Chemistry and Biochemistry and Center for Organic Photonics and Electronics, Georgia Institute of Technology, 901 Atlantic Drive, NW, Atlanta, GA 30332, USA
**joe.perry@chemistry.gatech.edu*

Abstract: Optical-quality, melt processable thick films of a conjugated polymer blend containing poly(2-methoxy-5-(2-ethyl-hexyloxy)-(phenylene vinylene)) (MEH-PPV), a C_{60} derivative (PCBM) and a plasticizer (1,2-di-*iso*-octylphthalate) have been developed and their nonlinear absorption and optical limiting properties have been investigated. These blend materials exhibited strong optical limiting characteristics in the near infrared region (750-900 nm), with broad temporal dynamic range spanning femtosecond to nanosecond pulse widths. The dispersion of the optical limiting figure-of-merit of the MEH-PPV:PCBM:DOP blend shows a peak near the wavelength of the MEH-PPV cation, indicating an important role of one-photon and two-photon induced charge transfer in the nonlinear absorption response.

OCIS codes: (160.0160) Materials; (160.4330) Nonlinear Optical Materials; (160.4890) Organic Materials; (190.0190) Nonlinear Optics; (190.4180) Multiphoton Processes; (190.4710) Optical Nonlinearities in Organic Materials.

References

1. J. E. Geusic, S. Singh, D. W. Tipping, and T. C. Rich, "3-photon stepwise optical limiting in silicon," Phys. Rev. Lett. **19**(19), 1126–1128 (1967).
2. J. W. Perry, K. Mansour, I. Y. S. Lee, X. L. Wu, P. V. Bedworth, C. T. Chen, D. Ng, S. R. Marder, P. Miles, T. Wada, M. Tian, and H. Sasabe, "Organic optical limiter with a strong nonlinear absorptive response," Science **273**(5281), 1533–1536 (1996).
3. L. W. Tutt, and A. Kost, "Optical limiting performance of C_{60} and C_{70} solutions," Nature **356**(6366), 225–226 (1992).
4. J. W. Perry, *Organic and metal-containing reverse saturable absorbers for optical limiters* (CRC Press INC, Boca Raton, FL, 1997).
5. G. S. He, C. Weder, P. Smith, and P. N. Prasad, "Optical power limiting and stabilization based on a novel polymer compound," IEEE J. Quantum Electron. **34**(12), 2279–2285 (1998).
6. G. S. He, L. X. Yuan, J. D. Bhawalkar, and P. N. Prasad, "Optical limiting, pulse reshaping, and stabilization with a nonlinear absorptive fiber system," Appl. Opt. **36**(15), 3387–3392 (1997).
7. P. F. Moulton, "Spectroscopic and laser characteristics of $TiAl_2O_3$," J. Opt. Soc. Am. B **3**(1), 125–133 (1986).
8. M. Cha, N. S. Saricftci, A. J. Heeger, J. C. Hummelen, and F. Wudl, "Enhanced nonlinear absorption and optical limiting in semiconducting polymer/methanofullerene charge transfer films," Appl. Phys. Lett. **67**(26), 3850–3852 (1995).
9. J. E. Ehrlich, X. L. Wu, I. Y. S. Lee, Z. Y. Hu, H. Röckel, S. R. Marder, and J. W. Perry, "Two-photon absorption and broadband optical limiting with bis-donor stilbenes," Opt. Lett. **22**(24), 1843–1845 (1997).
10. J. M. Hales, M. Cozzuol, T. E. O. Screen, H. L. Anderson, and J. W. Perry, "Metalloporphyrin polymer with temporally agile, broadband nonlinear absorption for optical limiting in the near infrared," Opt. Express **17**(21), 18478–18488 (2009).
11. J. W. Perry, S. Barlow, J. E. Ehrlich, A. A. Heikal, Z. Y. Hu, I. Y. S. Lee, K. Mansour, S. R. Marder, H. Rockel, M. Rumi, S. Thayumanavan, and X. L. Wu, "Two-photon and higher-order absorptions and optical limiting properties of bis-donor substituted conjugated organic chromophores," Nonlinear Opt. **21**, 225–243 (1999).
12. B. Kraabel, D. McBranch, N. S. Sariciftci, D. Moses, and A. J. Heeger, "Ultrafast spectroscopic studies of photoinduced electron transfer from semiconducting polymers to C_{60}," Phys. Rev. B **50**(24), 18543–18552 (1994).
13. C. J. Brabec, N. S. Sariciftci, and J. C. Hummelen, "Plastic solar cells," Adv. Funct. Mater. **11**(1), 15–26 (2001).

#118168 - $15.00 USD Received 12 Oct 2009; accepted 12 Nov 2009; published 17 Nov 2009

14. N. S. Sariciftci, L. Smilowitz, A. J. Heeger, and F. Wudl, "Photoinduced electron transfer from a conducting polymer to buckminsterfullerene," Science **258**(5087), 1474–1476 (1992).
15. D. Moses, A. Dogariu, and A. J. Heeger, "Mechanism of carrier generation and recombination in conjugated polymers," Synth. Met. **116**(1-3), 19–22 (2001).
16. T. Kato, T. Kodama, and T. Shida, "Electronic absorption spectra of the radical anions and cations of fullerenes: C_{60} and C_{70}," Chem. Phys. Lett. **180**(5), 446–450 (1991).
17. P. A. van Hal, M. P. T. Christiaans, M. M. Wienk, J. M. Kroon, and R. A. J. Janssen, "Photoinduced electron transfer from conjugated polymers to TiO," J. Phys. Chem. B **103**(21), 4352–4359 (1999).
18. S.-J. Chung, G. S. Maciel, H. E. Pudavar, T.-C. Lin, G. S. He, J. Swiatkiewicz, P. N. Prasad, D. W. Lee, and J.-I. Jin, "Two-photon properties and excitation dynamics of poly(*p*-phenylenevinylene) derivatives carrying phenylanthracene and branched alkoxy pendents," J. Phys. Chem. A **106**(33), 7512–7520 (2002).
19. A. Samoc, M. Samoc, M. Woodruff, and B. Luther-Davies, "Tuning the properties of poly(p-phenylenevinylene) for use in all-optical switching," Opt. Lett. **20**(11), 1241–1243 (1995).
20. A. Dogariu, D. Vacar, and A. J. Heeger, "Picosecond time-resolved spectroscopy of the excited state in a soluble derivative of poly(phenylene vinylene): Origin of the bimolecular decay," Phys. Rev. B **58**(16), 10218–10224 (1998).
21. L. Smilowitz, and A. J. Heeger, "Photoinduced absorption from triplet excitations in poly(2-methoxy-5-(2'-ethyl-hexyloxy)-*p*-phenylene vinylene) oriented by gel-processing in polyethylene," Synth. Met. **48**(2), 193–202 (1992).
22. K. Vandewal, A. Gadisa, W. D. Oosterbaan, S. Bertho, F. Banishoeib, I. Van Severen, L. Lutsen, T. J. Cleij, D. Vanderzande, and J. V. Manca, "The relation between open-circuit voltage and the onset of photocurrent generation by charge-transfer absorption in polymer: Fullerene bulk heterojunction solar cells," Adv. Funct. Mater. **18**(14), 2064–2070 (2008).
23. T. W. Ebbesen, K. Tanigaki, and S. Kuroshima, "Excited-state properties of C_{60}," Chem. Phys. Lett. **181**(6), 501–504 (1991).
24. T. Drori, C. X. Sheng, A. Ndobe, S. Singh, J. Holt, and Z. V. Vardeny, "Below-gap excitation of π-conjugated polymer-Fullerene blends: implications for bulk organic heterojunction solar cells," Phys. Rev. Lett. **101**(3), 037401–037404 (2008).
25. J. Nelson, "Diffusion-limited recombination in polymer-fullerene blends and its influence on photocurrent collection," Phys. Rev. B **67**(15), 155209–155218 (2003).
26. W. Holzer, A. Penzkofer, H. Tillmann, and H.-H. Hörhold, "Spectroscopic and travelling-wave lasing characterisation of gilch-type and horner-type MEH-PPV," Synth. Met. **140**(2-3), 155–170 (2004).
27. H. L. Chou, K. F. Lin, and D. C. Wang, "Miscibility and luminescence properties of MEH-PPV/DPO-PPV polyblends," J. Polym. Res. **13**(1), 79–84 (2006).
28. J. Shinar, Z. V. Vardeny, and Z. H. Kafafi, eds., *Optical and electronic properties of fullerenes and fullerene-based materials* (Marcel Dekker, Inc., New York, NY, 2000).
29. A. A. Bakulin, D. S. Martyanov, D. Y. Paraschuk, M. S. Pshenichnikov, and P. H. M. van Loosdrecht, "Ultrafast charge photogeneration dynamics in ground-state charge-transfer complexes based on conjugated polymers," J. Phys. Chem. B **112**(44), 13730–13737 (2008).
30. L. Goris, A. Poruba, L. Hod'akova, M. Vanecek, K. Haenen, M. Nesladek, P. Wagner, D. Vanderzande, L. De Schepper, and J. V. Manca, "Observation of the subgap optical absorption in polymer-fullerene blend solar cells," Appl. Phys. Lett. **88**(5), 052113 (2006).
31. Y. Lin, J. Zhang, L. Brzozowski, E. H. Sargent, and E. Kumacheva, "Nonlinear optical figures of merit of processible composite of poly(2-methoxy,5-(2'-(ethyl)hexyloxy)-*p*-phenylene vinylene) and poly(methyl methacrylate)," J. Appl. Phys. **91**(1), 522–524 (2002).
32. E. W. Van Stryland, Y. Y. Wu, D. J. Hagan, M. J. Soileau, and K. Mansour, "Optical limiting with semiconductors," J. Opt. Soc. Am. B **5**(9), 1980–1989 (1988).
33. H. Jiang, M. DeRosa, W. Su, M. Brant, D. McLean, and T. Bunning, "Polymer host materials for optical limiting," Proc. SPIE **3472**, 157–162 (1998).
34. R. C. Hollins, "Materials for optical limiters," Curr. Opin. Solid State Mater. Sci. **4**(2), 189–196 (1999).
35. A. Kost, L. Tutt, M. B. Klein, T. K. Dougherty, and W. E. Elias, "Optical limiting with $C_{(60)}$ in polymethyl methacrylate," Opt. Lett. **18**(5), 334–336 (1993).

1. Introduction

Materials with strong nonlinear optical absorption properties have long been recognized as potential optical limiting (OL) materials for applications such as sensor protection [1–4], noise reduction [5], and pulse shaping [6] in various wavelength regions. With the development of mode-locked and amplified Ti:Sapphire lasers [7], the need for effective optical limiters in the 700-1000 nm spectral range has increased. The essential requirements for OL materials are high linear transmission (T_0), low turn-on threshold (F_{Th}, defined here as the fluence where $T(F) = T_0/2$), high damage threshold, and large pulse energy suppression (S), which should be achieved over a wide spectral and temporal dynamic range (where S is defined as the

#118168 - $15.00 USD Received 12 Oct 2009; accepted 12 Nov 2009; published 17 Nov 2009

reciprocal of nonlinear transmittance, T_F, just before the damage threshold). A figure-of-merit (FOM) for evaluating the pulse suppression performance of an optical limiter is defined here as $FOM = T_0S = T_0/T_F$.

Several organic material systems utilizing different mechanisms for their nonlinear absorption (NLA) response have been reported previously [4,5,8–11]. Cha *et al.* reported on a blend of a conjugated polymer, poly(3-octyl thiophene) (P3OT), and a C_{60} fullerene derivative that was found to possess enhanced NLA and OL capability in the 700 – 950 nm range compared to the neat polymer or fullerene [8]. A nanosecond-pulse suppression of 9 dB (7.8X) was observed at 760 nm and was attributed to one-photon induced charge carrier absorption (CCA). The P3OT polymer functioned as a photoexcitable electron donor and the fullerene as an electron acceptor. The NLA was modeled and found to be enhanced due to CCA arising from fast and efficient charge transfer and charge separation, as well as relatively slow charge recombination [8,12]. However, the P3OT:fullerene blend exhibited low linear transmission (~0.45) resulting in a modest OL-FOM = 3.5.

One route to improving the linear transmission is to make use of two-photon absorption (2PA) as an excitation route, with photon energies lying below the linear absorption band edge [5,9–11]. However, because of the quadratic dependence of the excitation rate on intensity, purely 2PA-based systems are limited to use with relatively short pulse widths. With the contribution of subsequent absorption processes (e.g. excited state absorption, ESA, or CCA), the nonlinear attenuation can be dramatically increased [11] for longer (i.e. nanosecond) pulses, although the NLA response could diminish for yet longer pulses, depending on the timescale for relaxation of the excited state or charge recombination. While a recent report on a lead bis(ethynyl)porphyrin polymer material system exhibiting 2PA-induced ESA has shown promising broadband OL response at longer wavelengths (> 1050 nm) [10], 2PA-based systems in the current spectral region-of-interest (700-1000 nm) have resulted in OL-FOMs < 10 [9].

To develop an OL material in the near IR with improved linear transmittance and temporal dynamic range, a system with a combined contribution of 1PA- and 2PA-induced absorptions is of interest. In order to achieve such effective NLA, it is ideal to have spectral overlap of 1PA or 2PA with ESA or CCA in the spectral region-of-interest. If there is also spectral overlap of the 1PA and 2PA bands, both types of excitation can contribute to the induced absorption and can give rise to a nonlinear response over a wider temporal dynamic range. Furthermore, the states or species that contribute to the induced absorptions should be generated on a time scale much shorter than the pulse duration and the resulting excited states or carriers should have lifetimes comparable to or longer than the excitation pulse width. This is generally a difficult task to achieve in a single-component OL material.

In this paper, we report on the NLA and OL properties of blends of poly(2-methoxy-5-(2-ethyl-hexyloxy)-(phenylene vinylene)) (MEH-PPV), the fullerene (6,6)-phenyl-C_{61}-butyric acid methyl ester (PCBM), and a plasticizer known as di-octylphthalate (DOP). MEH-PPV/fullerene blends are well known to show efficient one-photon induced charge carrier generation and have been studied extensively as solar cell materials [13]. We recognized that the 2PA spectrum of MEH-PPV overlaps well with the MEH-PPV radical cation absorption, such that CCA should be induced and lead to strong NLA. To overcome poor optical quality and significant optical scattering in films of MEH-PPV and PCBM we investigated a ternary mixture comprising MEH-PPV, PCBM and DOP and were able to produce melt-processable, optical quality, thick films (25 μm) of this material. The results of linear spectroscopic studies, femtosecond-pulsed Z-scans, and OL measurements with both nanosecond and femtosecond laser pulses in the red-near IR (750-900 nm) will be described below.

#118168 - $15.00 USD Received 12 Oct 2009; accepted 12 Nov 2009; published 17 Nov 2009

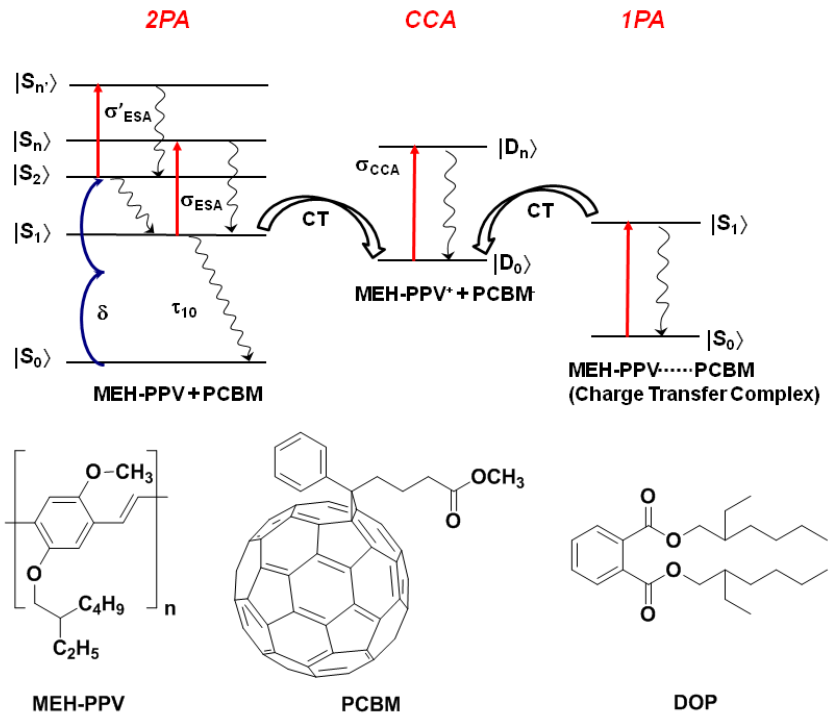

Fig. 1. Illustration of one- and two-photon induced excited state and charge carrier absorption in MEH-PPV:PCBM:DOP blends and the chemical structures of constituent compounds. The states illustrated represent only the MEH-PPV related electronic states in the system. The S symbols represent singlet states of MEH-PPV and MEH-PPV–PCBM charge transfer complex and the D symbols represent doublet states of the MEH-PPV radical cation.

2. MEH-PPV:PCBM:DOP blends

MEH-PPV:PCBM blends are interesting as potential nonlinear absorbing optical elements because of the linear and nonlinear absorption properties of MEH-PPV as well as the excited state and charge carrier absorption characteristics of both MEH-PPV and PCBM. Relative to P3OT, MEH-PPV has a larger bandgap (E_g) providing improved linear transmission in the near IR region. It has been shown that one-photon induced charge transfer can occur between MEH-PPV (electron donor) and PCBM (electron acceptor) leading to strongly absorbing charge carriers; the MEH-PPV cation shows a broad absorption band from 600 to 1100 nm and the PCBM anion shows absorption bands ranging from 850 to 1070 nm [12,14–17]. MEH-PPV has 2PA bands ranging from 750 to 900 nm [18,19] and ESA also in the near IR peaking at 1300 nm [20,21]. Furthermore, blends of MEH-PPV and PCBM have been shown to form ground-state charge transfer complexes (CTCs) that exhibit weak 1PA extending to wavelengths above the 1PA band edge of MEH-PPV [22]. Therefore, one-photon or two-photon excitation of the MEH-PPV:PCBM blend in the 700-900 nm range should lead to the generation of charge carriers [14,16,17] and/or excited states [20,21,23] that are strongly absorbing in the same wavelength range, as needed for effective NLA (see Fig. 1). The photoinduced charge transfer and separation have been reported to occur within 1 ps following excitation [24] in MEH-PPV:PCBM films, while the recombination of MEH-PPV cations and fullerene anions is slow (300 ns – 10 ms) [25]. For MEH-PPV, the singlet ESA lifetime is ~600 ps [20,21], which allows for efficient electron transfer quenching by PCBM. Thus, the combination of MEH-PPV and PCBM was investigated as a candidate OL material

#118168 - $15.00 USD Received 12 Oct 2009; accepted 12 Nov 2009; published 17 Nov 2009

that could have 2PA- and 1PA-induced ESA or CCA working together to contribute to effective OL in the same spectral range for various pulse durations.

3. Experiments

3.1 Sample preparation

MEH-PPV (M_n = 40,000-70,000, Sigma-Aldrich), poly(methyl methacrylate) (PMMA, M_n = 15,000, Sigma-Aldrich), PCBM (Sigma-Aldrich), and DOP (Sigma-Aldrich) were used as received. 25 μm thick films of three different compositions were fabricated for OL measurements and nonlinear spectroscopic characterization: (1) MEH-PPV:DOP (50%:50%, by weight) (2) MEH-PPV:PCBM:DOP (40%:10%:50%, by weight), and (3) PMMA:PCBM:DOP (35%:15%:50%, by weight). Each component was dissolved in spectroscopic-grade dichloromethane separately, and then the solutions were mixed to obtain the appropriate composition ratio by weight. Solvent was then removed under vacuum to obtain a homogenous mixture of the selected components. The dried mixtures were then transferred into an Ar-filled glove box and melted into films under inert atmosphere to avoid potential degradation at high temperature. To process the blend films, a hot plate was first preheated to the processing temperature (190-250°C). Then, the blend was sandwiched between thoroughly cleaned microscope glass slides and 25 μm thick PTFE spacers were used to control the film thickness. Next, the sandwiched sample was then placed on a preheated hot plate and a static compressive force was applied evenly to distribute the mixture. As soon as the sample had melted and flowed, the sandwiched film was immediately transferred onto a cold metal block (chilled in a −40°C freezer) and rapidly quenched. The fabricated blend films were then hermetically sealed with epoxy glue to avoid oxidation under ambient conditions.

Spin-coated films of MEH-PPV:DOP (100 nm thickness), MEH-PPV:PCBM:DOP (100 nm) and PMMA:PCBM:DOP (1.6 μm) were also prepared for linear spectroscopic measurements in order to observe distinct spectral features of the individual components. A 10-μm thick PMMA:PCBM:DOP was also prepared by drop-casting for observation of the weak absorption of PCBM in the 600 – 750 nm range. Film thicknesses were determined using a Dektak 6M contact profilometer.

3.2 Linear and nonlinear spectroscopic measurements

Linear transmission properties of blend films were determined by Vis-NIR linear absorption spectroscopy using a Shimadzu UV3100 UV-Vis-NIR spectrometer. The 2PA coefficients (β) of the blends were determined at 730 nm and 870 nm using the femtosecond-pulsed open-aperture Z-scan technique which has been described in detail elsewhere [10]. The instrumental accuracy associated with these measurements is estimated to be ± 15%.

3.3 Optical limiting

Optical limiting measurements were carried out with both femtosecond and nanosecond pulses to determine the power suppression capability of blends in the near IR region. The detailed experimental setup has been discussed in a previous publication [10], however a brief description will be given here. The nanosecond-pulsed OL measurements were performed using a flat top beam focused with an f/5 lens. The measurements were performed in the wavelength region from 750 – 900 nm with beam radii ($HW1/e^2$) measuring 30-40 μm at the sample position and pulse energies ranging from 5 nJ to 400 μJ. The femtosecond-pulsed OL measurements were performed using a Gaussian beam with radius of ~35 μm ($HW1/e^2$) at the sample position. The excitation wavelength of 810 nm was used with excitation energies from 0.5 to 1000 nJ.

#118168 - $15.00 USD Received 12 Oct 2009; accepted 12 Nov 2009; published 17 Nov 2009

4. Results and discussions

4.1 Formulation and processing of thick film conjugated polymer blends

The NLA of a blend material scales with the sample pathlength and the concentration of optically active chromophores within the sample. Moreover, the charge transfer efficiency depends on the distance between donors and acceptors in a blended solid film. Thus, considering these factors, the primary task in this study was to fabricate thick (> 15 μm) solid films of MEH-PPV and PCBM with high volume loading of the constituents, while maintaining optical transparency in the near IR. However, obtaining high optical quality, thick blend films involving conjugated polymers is rather challenging due to potential phase separation of components and degradation caused by high processing temperatures. These factors can lead to increased scattering and reduced linear transmittance in the films. Melt processing is often a viable route to the formation of optical quality glasses of polymers via rapid quenching of the melt. However, MEH-PPV has a high melting temperature (250-300 °C) [26,27], due to interchain interactions as is the case for many long-chain conjugated polymers, and was found to decompose before melting sufficiently for film processing. The addition of a plasticizer, such as DOP, dissolves and dilutes the polymer chains, and induces additional free volume in the blend which leads to a number of favorable characteristics: reduced melting and blend processing temperatures, improved processability and miscibility of the two component systems, and reduced crystallinity in the resulting films. Various ratios of DOP were investigated. Upon the addition of 50% DOP, the ternary DOP-containing blends could be processed at temperatures around 200-230°C. This permitted fabrication of optical quality films with thicknesses ranging from 15 – 200 μm and excellent transparency from 700 to 900 nm, while maintaining a high concentration of the polymer and fullerene (see Fig. 2 and Table 1).

4.2 Linear and Nonlinear absorption of MEH-PPV:DOP and MEH-PPV:PCBM:DOP Films

Figure 2 shows the linear absorption of thin and thick films of MEH-PPV:DOP, MEH-PPV:PCBM:DOP, and PMMA:PCBM:DOP. Spin-coated thin films of MEH-PPV:DOP and MEH-PPV:PCBM:DOP showed the electronic absorption peaks of MEH-PPV at 505 and 512 nm. The PMMA:PCBM:DOP thin film shows the expected electronic absorption bands for PCBM in the range of 400 to 750 nm, including a distinct weak band at 700 nm [28]. For the melt-processed thick films, the MEH-PPV:DOP film shows a sharp band edge at 625 nm. The film of the MEH-PPV:PCBM:DOP blend shows a weak absorption at ~700 nm, that we attribute to the PCBM, on top of an extended absorption tail below the band edge of MEH-PPV (out to ~870 nm) that likely results from the formation of a ground-state CTC [22,29,30]. Minor inhomogeneities were observed in optical microscopy, which might also contribute to some of the optical loss tail in the near IR. Such inhomogeneities may result from a small amount of crystallization of PCBM, as evidenced by the low density of very small crystallites in Fig. 2c.

Femtosecond-pulsed open-aperture Z-scan measurements (Table 1) yielded β values for MEH-PPV:DOP films which were found to be about half the reported value (80 cm/GW at 800 nm) of neat MEH-PPV [19,31], which is consistent with the ~50% dilution of MEH-PPV in the blend film. These 2PA coefficients are nearly an order-of-magnitude larger than for ZnSe, a wide bandgap semiconductor that has been used previously for OL in this spectral region [32]. Also, the values of β showed negligible intensity dependency in the irradiance range used, i.e. 1 – 12 GW/cm^2. While this result suggests that the dominant mechanism for NLA in MEH-PPV is 2PA, as might be expected in the femtosecond region, it does not preclude subsequent ESA of MEH-PPV at higher intensities. At 870 nm, the magnitudes of β were not significantly different for the MEH-PPV:DOP and MEH-PPV:PCBM:DOP films. At 730 nm, on the other hand, the value of β for MEH-PPV:PCBM:DOP showed a marked

#118168 - $15.00 USD Received 12 Oct 2009; accepted 12 Nov 2009; published 17 Nov 2009

difference relative to MEH-PPV:DOP, possibly indicating an additional pathway for NLA which could be due to the presence of CTCs leading to 1PA-induced ESA.

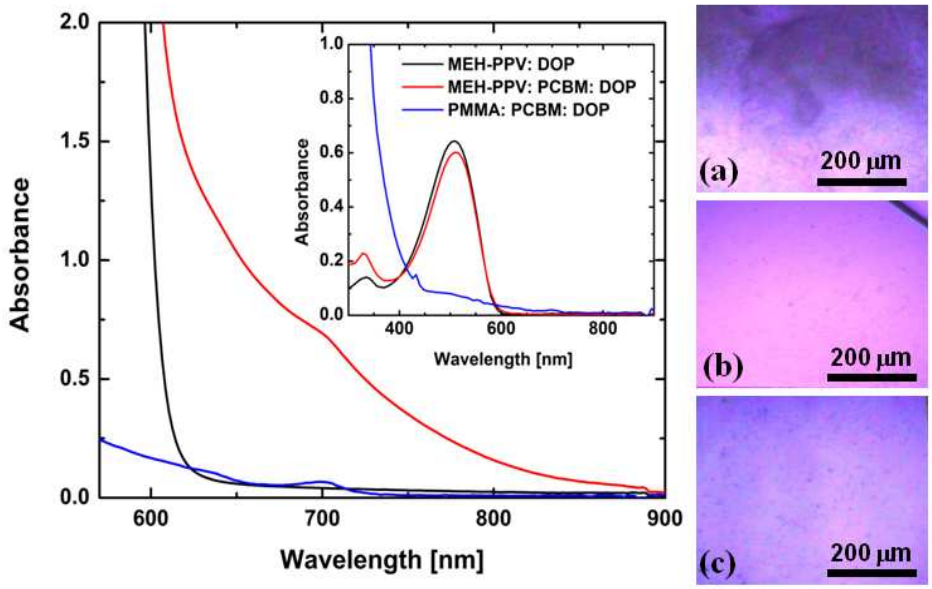

Fig. 2. (Left) Linear absorption spectra of melt-processed 25-μm thick MEH-PPV:DOP film (black) and MEH-PPV:PCBM:DOP (red) film and drop-cast 10 μm thick PMMA:PCBM:DOP (blue). Inset: Linear absorption spectra of spin-coated thin films of MEH-PPV:DOP (black, 100 nm), MEH-PPV:PCBM:DOP (red, 100 nm), and PMMA:PCBM:DOP (blue, 1.7 μm). (Right) Transmission optical microscopic images at 40X magnification of 25-μm thick melt-processed films of (a) neat MEH-PPV, (b) MEH-PPV:DOP, and (c) MEH-PPV:PCBM:DOP.

Table 1. Linear and nonlinear optical properties as well as optical limiting characteristics of blends examined.

Sample	T_0[a]	β [cm/GW]		ns-OL[b]		fs-OL[c]	
	800 nm	730 nm	870 nm	F_{Th} [J/cm^2]	*FOM*	F_{Th} [J/cm^2]	*FOM*
MEH-PPV:PCBM:DOP	0.76 ± 0.056	57	37	0.15	21	0.0019	9.7
MEH-PPV:DOP	0.90 ± 0.065	40 (955)[d]	33 (660)[d]	2.3	2.7	0.0021	8.2 (2.8)[e]
PMMA:PCBM:DOP	0.31 ± 0.084	-	-	4.3	2.4	0.03	1.1

[a] These are average values based on linear spectroscopic measurements on different spots for several films.
[b] Nanosecond OL with 4 ns, 830 nm pulses. The measurement uncertainty is ~ ± 15%.
[c] Femtosecond OL with 75 fs, 810 nm pulses. The measurement uncertainty is ~ ± 15%.
[d] The numbers in the parentheses are extracted 2PA cross-sections (δ). The conversion from 2PA coefficient (β) to δ is given as $\delta = \beta E_{ph}/N$, where N is the number density of MEH-PPV per repeat unit and E_{ph} is the photon energy of the excitation. The units of δ are 10^{-58} m^4·s·photon^{-1} (or GM).
[e] MEH-PPV:DOP showed minor, non-catastrophic damage at 4×10^{-3} J/cm^2 giving a FOM of ~2.8. However, the suppression capability of MEH-PPV:DOP continued until ~2×10^{-2} J/cm^2 giving a FOM of ~8.2.

#118168 - $15.00 USD Received 12 Oct 2009; accepted 12 Nov 2009; published 17 Nov 2009

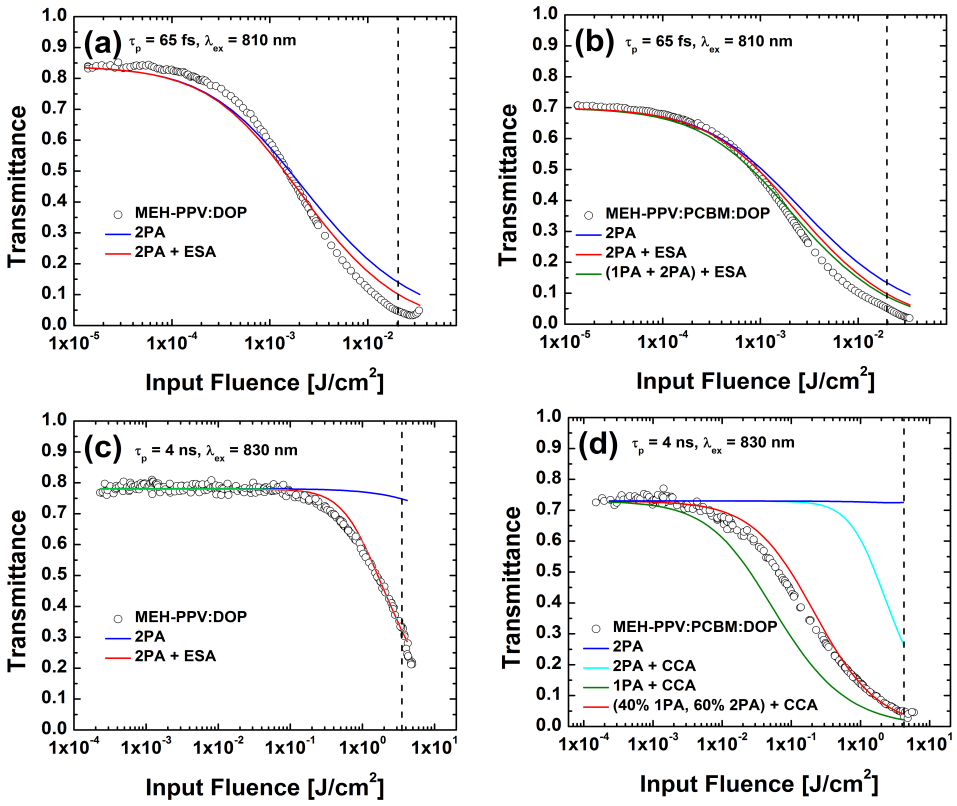

Fig. 3. Optical limiting data and numerical simulations for the 25 μm thick MEH-PPV:DOP and MEH-PPV:PCBM:DOP films. Femtosecond-pulsed (HW1/e ~65 fs) OL on MEH-PPV:DOP (a) and MEH-PPV:PCBM:DOP (b) at 810 nm. Nanosecond-pulsed (HW1/e ~4 ns) OL on MEH-PPV:DOP. (c) and MEH-PPV:PCBM:DOP (d) at 830 nm. Parameters for the numerical simulations are described in the text. Dashed lines mark the onset of damage.

4.3 Optical limiting performance of MEH-PPV based blends

Given the successful fabrication of thick, optical quality films of MEH-PPV based blends with strong NLA properties, femtosecond- and nanosecond-pulsed OL studies were undertaken to determine the pulse suppression efficacy of the films. As indicated in Table 1 and Fig. 3, MEH-PPV:DOP and MEH-PPV:PCBM:DOP showed significant differences in nanosecond-pulsed OL performance while the suppression behavior is similar when using femtosecond pulses. With femtosecond-pulsed excitation, MEH-PPV:DOP and MEH-PPV:PCBM:DOP both showed a similar turn-on threshold and pre-damage suppression, i.e. 10 dB (9X). Optical damage occurred at ~0.01 J/cm^2 under femtosecond pulse excitation for both MEH-PPV:DOP and MEH-PPV:PCBM:DOP, although MEH-PPV:DOP showed signs of minor, non-catastrophic damage at lower input fluences (see Table 1 and Fig. 3). With nanosecond-pulsed excitation, MEH-PPV:DOP showed a limited pulse suppression, 5 dB (3X), and a high turn-on threshold (F_{Th}, defined here as the fluence where $T(I) = T_0/2$) of 2.3 J/cm^2, while MEH-PPV:PCBM:DOP exhibited a F_{Th} of 100 times lower than MEH-PPV:DOP and a suppression that was 10 times higher (15 dB, 30X). Such a large suppression by MEH-PPV:PCBM:DOP exceeds the reported value achieved previously with a P3OT:fullerene blend [8]. Furthermore, by virtue of the improved linear transmittance of the MEH-PPV:PCBM:DOP blend, the peak OL-FOM (at 800 nm) shows nearly a 7-fold enhancement over the P3OT:fullerene blend [8]. Interestingly, the damage thresholds of the blend films

#118168 - $15.00 USD Received 12 Oct 2009; accepted 12 Nov 2009; published 17 Nov 2009

containing DOP are relatively large under nanosecond pulse exposure, 3.5 – 4.2 J/cm^2. These values are comparable to some of the larger values reported in the literature for dye doped polymers, such as metallophthalocyanine doped polymethylmethacrylate [2]. The high damage thresholds of the DOP based blends are likely the result of the viscoelastic gel-like behavior of the blends. High damage thresholds have previously been reported for elastomeric and viscoelastic gel hosts containing nonlinear optical dyes [33–35]. Such gel-like solid solutions are able to better dissipate the shocks associated with high fluence exposures and recover from transient deformations as compared to stiffer host materials.

The differences in OL behavior between the femtosecond and nanosecond pulsed excitation for MEH-PPV:DOP and MEH-PPV:PCBM:DOP indicates that the NLA mechanisms contributing to the suppression are likely different in these two temporal regimes. For the MEH-PPV:DOP film, since MEH-PPV is the only active nonlinear absorbing chromophore, the dominant mechanisms for NLA are primarily 2PA and ESA in both femtosecond and nanosecond regimes. For MEH-PPV:PCBM:DOP however, charge carrier generation and absorption could contribute to the NLA mechanism, especially for nanosecond pulse durations. As evidenced by the poor OL suppression of the PMMA:PCBM:DOP control film in both temporal regimes, direct excitation of PCBM alone by either 1- or 2-PA likely provides a negligible contribution to the NLA of the blend. For femtosecond-pulsed excitation, the timescale for charge transfer and separation of charge carriers (~1 ps for MEH-PPV:PCBM [24]) is longer than the duration of the pulse width, therefore it is likely that ESA following excitation of MEH-PPV is still the primary route for NLA. This is consistent with the similar OL suppression observed for MEH-PPV:PCBM:DOP and MEH-PPV:DOP. On the other hand in the nanosecond regime, charge transfer occurs essentially instantaneously with respect to the pulse width which, coupled with the lifetime of the charge carriers (i.e. up to 3 ms [25]), suggests that induced CCA would be the dominant NLA mechanism. Furthermore, the turn-on threshold for MEH-PPV:PCBM:DOP is much lower (Fig. 3d) than that of MEH-PPV:DOP. Such a low threshold indicates an additional excitation pathway different from 2PA may provide a significant contribution. Since PMMA:PCBM:DOP showed negligible suppression, this additional pathway could be attributed to CTC absorption and, given its spectral overlap with MEH-PPV 2PA, it is likely that the large OL suppression of MEH-PPV:PCBM:DOP benefits from a combination of 1PA and 2PA excitation processes (Fig. 1). In order to understand and distinguish the contributions of 2PA (MEH-PPV) and 1PA (CTC) in the NLA response of MEH-PPV:PCBM:DOP, wavelength-dependent OL studies and numerical simulations of the OL data were carried out and are discussed below.

4.4 Dispersion of NLA

Wavelength-dependent OL studies of the MEH-PPV:DOP and MEH-PPV:PCBM:DOP blends were performed with nanosecond pulses in the 750 – 900 nm region. As shown in Fig. 4, MEH-PPV:PCBM:DOP has a considerably larger OL-FOM than MEH-PPV:DOP, particularly at shorter wavelengths. The dispersion of the OL-FOM for MEH-PPV:PCBM:DOP shows a peak at ~800 nm and monotonically decreases going towards 900 nm. The large suppression at shorter wavelengths again suggests a contribution from CTC absorption. At longer wavelengths, where CTC absorption is diminished, the 1PA contribution is reduced and 2PA-induced CCA dominates. Therefore, at shorter excitation wavelengths, the suppression mechanism in MEH-PPV:PCBM:DOP is likely due to both 1PA- and 2PA-induced CCA. While MEH-PPV:PCBM:DOP showed similar suppressions from 750 to 830 nm, the FOMs were found to be optimal at 800 nm (FOM ~23) and 830 nm (FOM ~21) as a result of the compromise between linear transmission loss and pulse suppression.

#118168 - $15.00 USD Received 12 Oct 2009; accepted 12 Nov 2009; published 17 Nov 2009

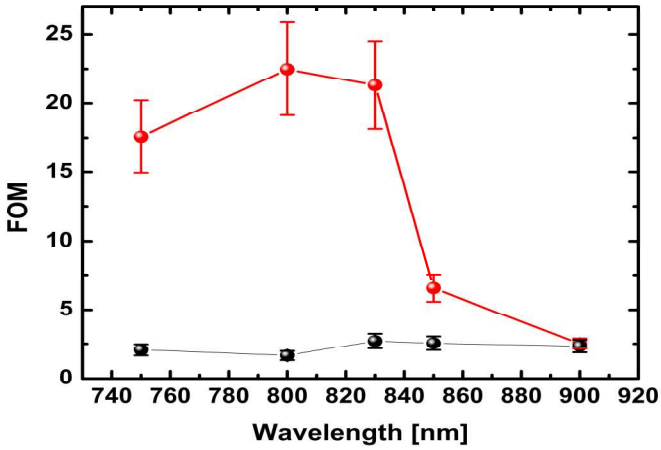

Fig. 4. Wavelength-dependence of FOM for nanosecond-pulse OL of 25 μm thick films of MEH-PPV:DOP (black) and MEH-PPV:PCBM:DOP (red) blends.

4.5 Numerical simulations of optical limiting

A method for nonlinear beam propagation (see ref [10]. for details) was employed to simulate the OL data in both femtosecond and nanosecond regimes in order to better understand the potential mechanisms contributing to the pulse suppression. Figure 3 shows these simulations alongside the experimental data for MEH-PPV:DOP and MEH-PPV:PCBM:DOP. Experimentally-determined beam profile and pulse shape parameters were used in the simulations as were sample-specific parameters (e.g. film thickness, concentration, linear transmittance, etc.). Parameters such as ESA and CCA lifetimes and charge transfer rates were adopted from the literature values (see Section 2 above). The 2PA cross-section was estimated to be ~780 GM in the 810-830 nm range based on the femtosecond Z-scan results (see Table 1). Consequently, the MEH-PPV ESA cross section became the only free fitting parameter when simulating the nanosecond-pulsed OL of the MEH-PPV:DOP film at 830 nm. The extracted value for the cross section was found to be $\sigma_{ESA} = 1.1 \times 10^{-20}$ m^2 at 830 nm, which is very similar to the value at 775 nm reported in the literature [20]. It should be noted that the MEH-PPV ESA was modeled as a single effective excited state absorption, although $S_2 \rightarrow S_n$, and $S_1 \rightarrow S_n$ absorption processes could contribute on short timescales. Figure 3c shows that 2PA itself has a negligible contribution to the nanosecond OL without including the subsequent ESA. This simulation as well as the absence of any appreciable 1PA for MEH-PPV:DOP in this spectral region validates the use of the 2PA-induced ESA process. The same NLA mechanism was used to simulate the femtosecond OL data in Fig. 3a. The simulations closely follow the experimental data, although it is clear that 2PA itself plays the predominant role in the pulse suppression for this temporal regime.

As discussed above, the same NLA mechanism responsible for the femtosecond OL response in MEH-PPV:DOP should also be responsible for the pulse suppression in MEH-PPV:PCBM:DOP. This is confirmed in Fig. 3b where 2PA is shown to be prominent in the nonlinear response of the blend. Not surprisingly, including 1PA as an additional excitation process (due to CTC absorption) showed only moderate improvement in the femtosecond OL response. For the nanosecond OL simulations of MEH-PPV:PCBM:DOP, the CCA cross section was extracted from the data taken at 900 nm. Since the contribution from CTC absorption is negligible at this wavelength, a 2PA-induced CCA model could be employed. The extracted cross section value was $\sigma_{CCA} = 1.3 \times 10^{-21}$ m^2 which is quite similar to the value found previously for the MEH-PPV cation [17]. This is consistent with transient absorption

#118168 - $15.00 USD Received 12 Oct 2009; accepted 12 Nov 2009; published 17 Nov 2009

data taken on MEH-PPV:PCBM blends [24], which show the MEH-PPV cation plays a dominant role in the CCA following excitation. Furthermore, the dispersion of the OL-FOM shown in Fig. 4 is also reminiscent of the MEH-PPV cation spectrum. With the value of σ_{CCA} (scaled according to the cation spectrum at the appropriate wavelength), nanosecond-pulsed OL could be simulated for the 830 nm data. It is clear from Fig. 3d that the mechanism of 2PA-induced CCA does not achieve the observed pulse suppression. However, 1PA-induced CCA (via the ground-state CTC) overestimates the suppression. Only by assuming a fractional contribution from both the CTC absorption and MEH-PPV 2PA (40% 1PA-CCA and 60% 2PA-CCA) could the data be reliably simulated. This is entirely consistent with the notion that only a fraction of the MEH-PPV units form CTCs while the remaining population exists as uncomplexed sub-units. Consequently, the OL response of MEH-PPV:PCBM:DOP results from a combination of both 1PA- and 2PA-induced CCA which is consistent with the results from the OL-FOM dispersion studies.

5. Conclusion

In summary, a ternary mixture including a conjugated polymer electron donor, a fullerene electron acceptor and a plasticizer allowed for the fabrication of an optical quality, thick film of a MEH-PPV:PCBM:DOP blend for optical limiting. In the femtosecond regime, two-photon absorption induced excited state absorption of MEH-PPV dominated the suppression and ~10 dB of suppression was observed for both MEH-PPV:DOP and MEH-PPV:PCBM:DOP blends. In the nanosecond regime, the suppression was enhanced by the accumulation of absorbing charge carriers over the long pulse duration and a contribution of one-photon absorption to the carrier generation due to a ground-state charge-transfer complex of MEH-PPV and PCBM, especially at the shorter wavelengths studied. MEH-PPV:PCBM:DOP showed a significantly reduced turn-on threshold and increased suppression of 15 dB, relative to MEH-PPV:DOP. The MEH-PPV:PCBM:DOP blend showed stronger suppression than what has been reported to date for organic optical limiters in the 750-900 nm range [5,8,9,11] and thus has potential as an efficient optical limiting material in the femtosecond to nanosecond temporal range for near IR wavelengths.

Acknowledgements

This material is based upon work supported in part by the DARPA MORPH Program and ONR (N00014-04-0095 and N00014-06-1-0897) and the STC Program of the National Science Foundation under Agreement Number DMR-0120967.

#118168 - $15.00 USD Received 12 Oct 2009; accepted 12 Nov 2009; published 17 Nov 2009